VIA MEDICA

Review article

NOWOTWORY Journal of Oncology
2018, volume 68, number 4, 184–196
DOI: 10.5603/NJO.2018.0030

ISSN 0029–540X
www.nowotwory.edu.pl

Methods of anatomical and metabolic imaging in head and neck region tumors

Natalia Samołyk-Kogaczewska[1], Ewa Sierko[1, 2], Marek Z. Wojtukiewicz[2]

The incidence of head and neck cancer (HNC) ranges from 5.5% to 6.2% of general cancer incidence in Poland as well as in other European countries and in the US. Precise evaluation of the clinical stage in this group of patients allows for personalized treatment, *inter alia*, to choose proper surgery technique, to plan and verify radiation therapy. It is a result of availability of wide spectrum of imaging methods currently used in oncology. These methods are also used in the suitable assessment of antineoplastic therapy effects, which gives the chance of early detection of cancer progression. Methods of imaging diagnostics — anatomical and metabolic — differ in terms of sensitivity, specificity and diagnostic accuracy. Each of them has advantages and disadvantages in imaging of HNC, hence, choice of treatment method should not be made based on single imaging modality. Increasingly, information obtained from alternative imaging studies support optimal decision in everyday clinical practice.

This review describes clinical usefulness of currently available morphological and metabolic imaging methods in HNC patients, with particular emphasis on innovative technologies, like PET/MR hybrid.

NOWOTWORY J Oncol 2018; 68, 4: 184–196

Key words: diagnostic imaging, molecular imaging, head and neck cancer, positron-emission tomography, PET/MR

Introduction

Head and neck cancers (HNC) are a significant clinical and social problem. In Poland, the incidence of HNC (except for thyroid cancer) in recent years ranges from 5.5% to 6.2% of the total number of cases of malignant tumors. Similar incidence rates also apply to other European countries and the United States [1]. Accurate assessment of the clinical stage in this group of patients is essential to select the best treatment strategy. The challenge is not only to define precisely the T and N parameters (according to TNM classification), but also to detect possible metastatic lesions and identify the primary lesion in patients with initially diagnosed lymph node metastases [2]. Currently we have a variety of head and neck imaging methods available, such as ultrasonography (USG), X-ray, computed tomography (CT), magnetic resonance imaging (MRI), positron emission tomography (PET) using various radiotracers — integrated with CT or MRI. Dynamic technological development of these methods has been observed for years. Each of them has its own strengths and weaknesses in imaging diagnostics, but the right choice of these examinations allows to find answers to clinical questions about the location and grade of the cancer. Increasingly common information obtained thanks to them supports making the right therapeutic decision, precise implementation of medical procedures (e.g. scope of surgeries, radiotherapy) and monitoring of treatment results.

Ultrasonography

Ultrasound examination is a commonly used technique in clinical practice. This method is best suited for the diagnosis of cervical lymph nodes [2, 3]. The sensitivity of this

[1]Department of Radiotherapy, Comprehensive Cancer Center in Białystok, Poland
[2]Department of Oncology, Medical University of Białystok, Poland

examination oscillates around 94%, its specificity — 77% [4–7]. Ultrasound can detect pathologies such as necrosis or microcalcifications in lymph nodes of normal size. It is possible to distinguish inflammatory lymphadenopathy from metastatic lymph nodes, e.g. by finding differences in vascularity and blood flow observed with color Doppler ultrasound [3, 8]. The size of the lymph node, its shape, echogenicity, structure and image of the hilum are assessed on a gray scale. An enlarged (> 10 mm), reactive lymph node is usually oval in shape, its echogenicity is reduced, structure is uniform and hilum is clearly marked. A neoplastic lymph node is round-shaped, with heterogeneous structure, invisible nodal hilum and decreased echogenicity [3]. Lymph nodes are evaluated and measured in real time, which accelerates the diagnosis and introduction of possible treatment [9]. An additional option of ultrasound imaging, i.e. elastography, allows to show the cohesiveness of the evaluated tissues with a color scale — lesions with a greater cohesiveness may suggest a neoplastic background. Modern ultrasound devices provide high quality images, making this examination one of the basic tools for soft tissues and superficial organs imaging [3]. On the other hand, lymph nodes of some groups lying deeper are beyond the scope of the examination, e.g. retropharyngeal lymph nodes (group VII), which may be the location of metastases from the nasal and the oral pharynx [8].

Ultrasound examination can also be used in the evaluation of tumor (T parameter according to TNM) in oral cavity cancers, most often tongue cancers. For this purpose, a suitable intraoral ultrasonography (IOUS) probe is used, which allows to assess the thickness of the infiltration and the structure of cancer tissue [10]. Ultrasonography is also a commonly used method in the diagnosis of secondary focal abnormalities in the liver, which is the third most frequent localization of HNC distant metastases [11, 12]. The sensitivity of liver metastatic lesions detection can be increased by 30–40% due to the administration of ultrasound contrast agents. They consist of microbubbles of air suspended in human albumin or galactose solution, and their presence in the vessels of the examined tissue amplifies the signal returning to the receiver in the probe [13]. The advantage of ultrasound techniques over other imaging methods is low examination costs and wide access to ultrasound devices. Ultrasonography is often used in post-treatment follow-up of HNC patients, especially in follow-up examinations of the regional lymphatic system [14]. Sensitivity and specificity of ultrasound examinations in diagnostics of local and regional recurrence is high and amounts to 81% and 87%, respectively [15]. In addition, ultrasound plays a key role during imaging-guided biopsy, as it enables the selection of the optimal place from which the material will be collected, allowing for histopathological verification of the lymph node or superficially located tumor detected by examination [2]. However, the basic limitation of this method is that the precision of the study result depends on the experience and manual skills of the doctor performing the examination [8].

Ultrasound evaluation is also used in IGRT (image-guided radiation therapy), where it is adapted to verify the position of the patient with highly specialized RT techniques [16, 17]. Ultrasound allows to monitor changes in the structure of salivary glands under the influence of X-rays during RT in HNC, which in the future may result in better protection of the salivary glands and prevention of xerostomia [18].

X-ray

X-rays are the most available and cheapest imaging method [19]. Currently, the number of indications for the use of X-ray examination in HNC diagnostics has decreased due to the development of such imaging techniques, as CT or MR.

An X-ray examination in the form of a dental panoramic radiograph makes it possible to visualize the neoplastic infiltration in the mandible or bone structures of the ethmoido-maxillary massif in the case of advanced cancers of these regions [20, 21]. In addition, a dental panoramic radiograph performed before the start of radiation therapy (RT) in the head and neck region also serves to assess the condition of the dentition and to identify possible odontogenic foci, thus supporting a dentist's decisions during oral cavity sanitation before RT [22, 23].

On the other hand, X-ray examination in Waters view (an occipitomental view) is a baseline study in diagnostics of facial pathology. An X-ray taken in this way is a summary projection of the head structures, which makes it possible to assess only large sinuses: frontal and maxillary, namely: the level of fluid in the sinuses, significant thickening of the mucous membranes, the location of polyps and abnormal aeration of the sinuses [16, 24].

In X-ray examinations, a characteristic phenomenon is the formation of high contrast between bone tissue and surrounding soft tissues, which is related to the different chemical structure of these tissues and the physical interaction of X-rays with the matter. The lack of these differences between the soft tissues makes it very difficult to obtain a clear contrast in an X-ray image. Therefore, X-rays are unsuitable for soft tissue imaging in HNC, including lymph nodes, where CT and MR are the most important [19]. However, in terms of bone system diagnostics, X-ray is the "gold standard" and the most frequently performed examination used to assess metastatic lesions to bones or their direct infiltration by a tumor developing nearby [25]. Lesions like "pepper pot skull" or "raindrop skull" (lesions resembling an image of a raindrop splashing against the ground) — symptoms characteristic of multiple myeloma lesions in the skull bones, also can be observe during imaging the head region using X-ray [26, 27].

X-ray except the bone structures allows for good visibility of pulmonary tissue [19]. It is often used to detect

possible HNC metastatic lesions in the lungs or synchronous lung cancer. This examination carried out in two projections (anterior-posterior and lateral) is a minimum in terms of the assessment of the M parameter (according to TNM) in the chest area [20]. However, in comparison to the "gold standard" of CT in chest region diagnostics, X-ray examination is burdened with a significant percentage of false negative results [28].

X-ray images are also used during the initial simulation, which is the stage of radiotherapy planning. X-ray allows to localize neoplastic lesions, as well as to predefine the geometry of the radiation beam, including the shape and position of therapeutic fields with simple two-dimensional RT planning. However, increasingly X-ray is replaced by a simulation with the CT device [29].

X-ray images are also used to verify the position of the patient before starting the radiotherapy — these are the so-called portal images taken in the linear accelerator room with a megavolt photon beam. In next step they are compared with 2D images documenting the position of the patient, obtained during the initial simulation in the simulator's room [30].

A more modern method of verifying a patient positioning based on X-ray images is EPID (electronic portal imaging device) — a system for portal imaging that records X-ray images in an electronic form. EPID is a more accurate method, which also allows for *in vivo* measurements [31, 32]. X-ray position verification is used not only in the case of photon beam radiotherapy, but also in proton therapy [33]. Currently, more and more technologically advanced systems are being constructed to verify the position of a patient — not only before the start of treatment, but also during each RT fraction. One of such systems is BrainLab's ExacTrac®, consisting of an infrared optical positioning system (ExacTrac) — for pre-setting and precise motion control of the therapeutic couch and a kV-based X-ray imaging system (X-ray 6D) to verify a patient's position. The X-ray 6D system consists of two X-ray radiation sources placed in the floor, which emit slanting X-ray beams intersecting in the isocenter, received by compatible detectors mounted on the ceiling. The 6D fusion software generates sets of digital radiograms based on three axes (x, y, z) and three different angles (obtained by moving the couch). The image sets are automatically, in real time, matched with the CT performed for RT planning. The obtained shifts values are transferred on-line to the patient's positioning system, which automatically introduces changes to the patient's position. The ExacTrac® system is used in patient positioning during highly specialized radiotherapy procedures such as IMRT (intensity modulated radiotherapy) or SRT/SBRT (stereotactic radiotherapy/stereotactic body radiotherapy), performed in the head and neck area [34–36].

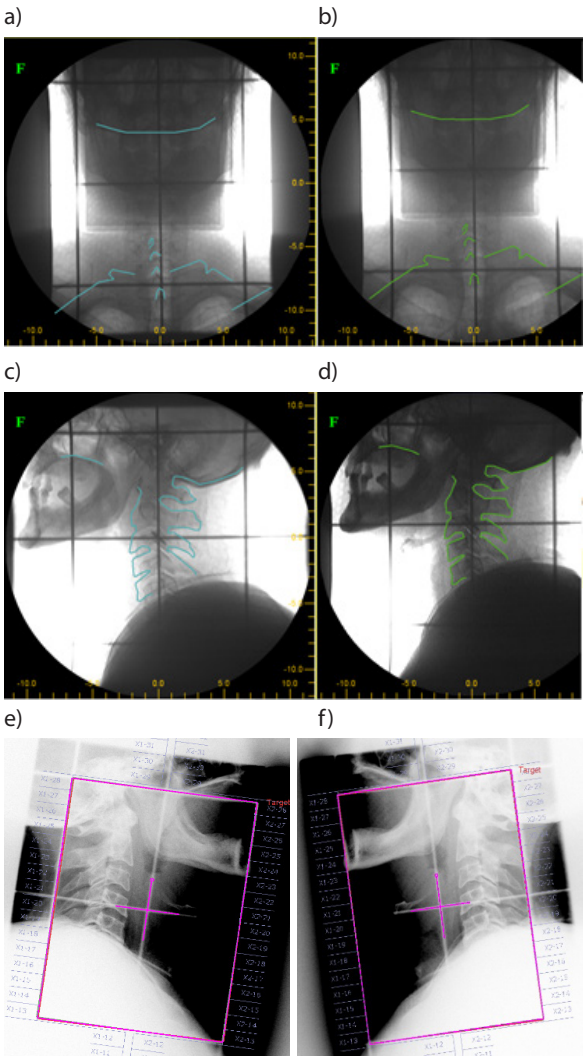

Figure 1. Use of X-ray images to verify a patient's positioning before starting radiation therapy (**a**, **b**, **c**, **d**) and in two-dimensional planning (2D) of radiation therapy (**e**, **f**). Photographs a and c are reference images, while photographs b and d are verification images. In order to determine the mutual position of the fields in both pictures, the same anatomical structures were marked. The next step is to superimpose the images on each other and read the shifts along the x, y, z axes

Computed tomography

Computed tomography (CT) is a recognized and widely used method allowing for spatial imaging of head and neck region tissues. In CT devices, the X-ray tube emitting X-rays moves around the examined object, and the changes in the intensity of radiation after passing through the patient's body are recorded with the use of detectors located on the periphery of the device. Afterwards, the received measurement values are processed electronically and an image reconstruction is obtained [13]. The features of the primary neoplasm (location, dimensions, infiltration on adjacent structures, presence of necrosis) of other head and neck organs for the presence or exclusion of a second, independent tumor and the condition of regional lymph nodes are

routinely assessed in CT [14]. The CT examination is characterized by lower accuracy of soft tissue imaging, where MR has a significant advantage, however, bone structures and cartilage tissue, e.g. thyroid cartilage, are very well visible [8]. Therefore, it is possible to detect the infiltration of these structures by the cancer. Determination of bone or cartilage infiltration significantly influences therapeutic decisions. This method is also a useful tool in determining the stage of N parameter (according to TNM). In the meta-analysis carried out by Sung et al. [37] higher sensitivity of CT (84%) vs MR (80%) in the detection of enlarged lymph nodes, with lower specificity of CT examination (72% vs 81%) was proven.

In the group of patients with HNC, the lungs are the most frequent location of metastases, as well as the second independent tumor [2, 11]. The CT examination is an effective method of imaging of pulmonary tissue pathology, hence its well-established place in the protocols for determining the clinical advancement stage in patients with HNC [2, 8]. The second most frequent location of HNC metastases are bones [11]. Among the imaging techniques in this case the CT is of great importance. This examination has a significant advantage over X-rays, especially in diagnostics of lesions in flat bones and complex bones (pelvic bones, scapula, vertebral column, ribs), which are usually not sufficiently clear on X-ray images. The CT makes it possible to assess the depth of cancer infiltration in individual parts of the bone: the cortical layer and the cancellous bone. 3D reconstruction of CT images helps to diagnose superficial bone lesions. The CT shows the damage of the bone structure by cancer, bone fractures, mineralization of the bone matrix and periosteal lesions better than the MR [25].

Despite its limitations, CT is often used especially in diagnostics before therapy [9]. However, the examination requires the administration of an intravenous iodine contrast agent, which visualizes vascular structures and thus provides more information. HNCs are well vascularized, so the contrast allows for better imaging (contrasting) [8, 38]. Analysis comparing CT scan with intravenous contrast and PET/CT scan for metastatic lymph node detection in preoperative management in patients with HNC did not show statistically significant differences in sensitivity of both examinations, however, it indicated at a higher specificity of CT with contrast [39]. Taghipour et al. [40] demonstrated that CT with contrast and PET/CT have a similar precision in the assessment of the primary neoplasm site in the local and regional assessment of patients with squamous cell carcinoma of the oropharynx after radical treatment.

The use of iodine-contrasting agents may result in the occurrence of certain undesirable side effects. One of them is renal damage (CIN — contrast-induced nephropathy), with decrease in glomerular filtration rate as the main symptom. Chronic renal disease and diabetic nephropathy are particular risk factors for CIN. Other factors increasing the probability of post-contrast nephropathy are dehydration, severe heart failure, diuretics and nonsteroidal anti-inflammatory drugs. The adverse effects on the kidneys depend on the osmolarity, dose and route of administration of the contrast agent and on the time elapsed since the previous examination with this type of substances. The biggest negative impact on kidneys is observed in the case of contrasting medium of high osmolarity (1400–2100 mOsm/kg), which are rarely used now. Lower risk (5–10 times) is associated with the administration of low osmolarity (500–800 mOsm/kg) and isosmotic (290 mOsm/kg) agents. Other side effects associated with the use of iodine contrast substances are allergic reactions. Patients with a history of moderate to severe allergic reaction to contrast media, bronchial asthma and allergies requiring treatment are particularly at risk. The use of a highly osmotic agent also increases the risk of this type of reaction. The administration of iodine contrast media is contraindicated in patients with evident hyperthyroidism (e.g. untreated Graves-Basedow disease, toxic multinodular goiter) due to the high risk of thyrotoxicosis [41].

A certain burden on the patient with CT is the dose of ionizing radiation that he or she receives during the entire examination. According to the FDA (Food and Drug Administration), the individual risk associated with a CT scan, necessary in a given clinical situation, is relatively low compared to the benefits brought by adequate diagnostics [42]. Another CT deficiency is the occurrence of artifacts, the source of which are dental fillings and implants, obscuring the structures of the oral cavity and partially of the oropharynx [2]. New algorithms are being developed in tomographs' software in order to eliminate the impact of artifacts on the image. It also helps to reduce the effect of the mobility of anatomical structures during breathing and swallowing, especially in patients who have problems with lying motionless for a long time [8].

CT scan after intravenous contrast agent administration is the basis for planning radiotherapy, one of the main methods of HNC treatment [2, 14]. The obtained CT images are sent to computer software used for treatment planning, where the radiotherapist determines, directly on CT scans, the volume of the tumor, nodal areas, tumor or nodal bed, metastatic focus and healthy organs [43]. CT imaging is also used in the process of verifying the position of the patient before radiotherapy starting, especially in the case of radiotherapy techniques requiring precise location of the irradiated area, i.e. SBRT or IMRT. Among the tools used for this purpose, these are the most common in clinical practice: CT-on-rails (a tomograph moving on rails in a therapeutic device room), kV CBCT (cone beam computed tomography), where the radiation beam originates in a X-ray tube attached to the arm of the radiotherapy device) and MV CBTC (CBCT using a megavolt beam generated by a linear accelerator) [34, 44, 45].

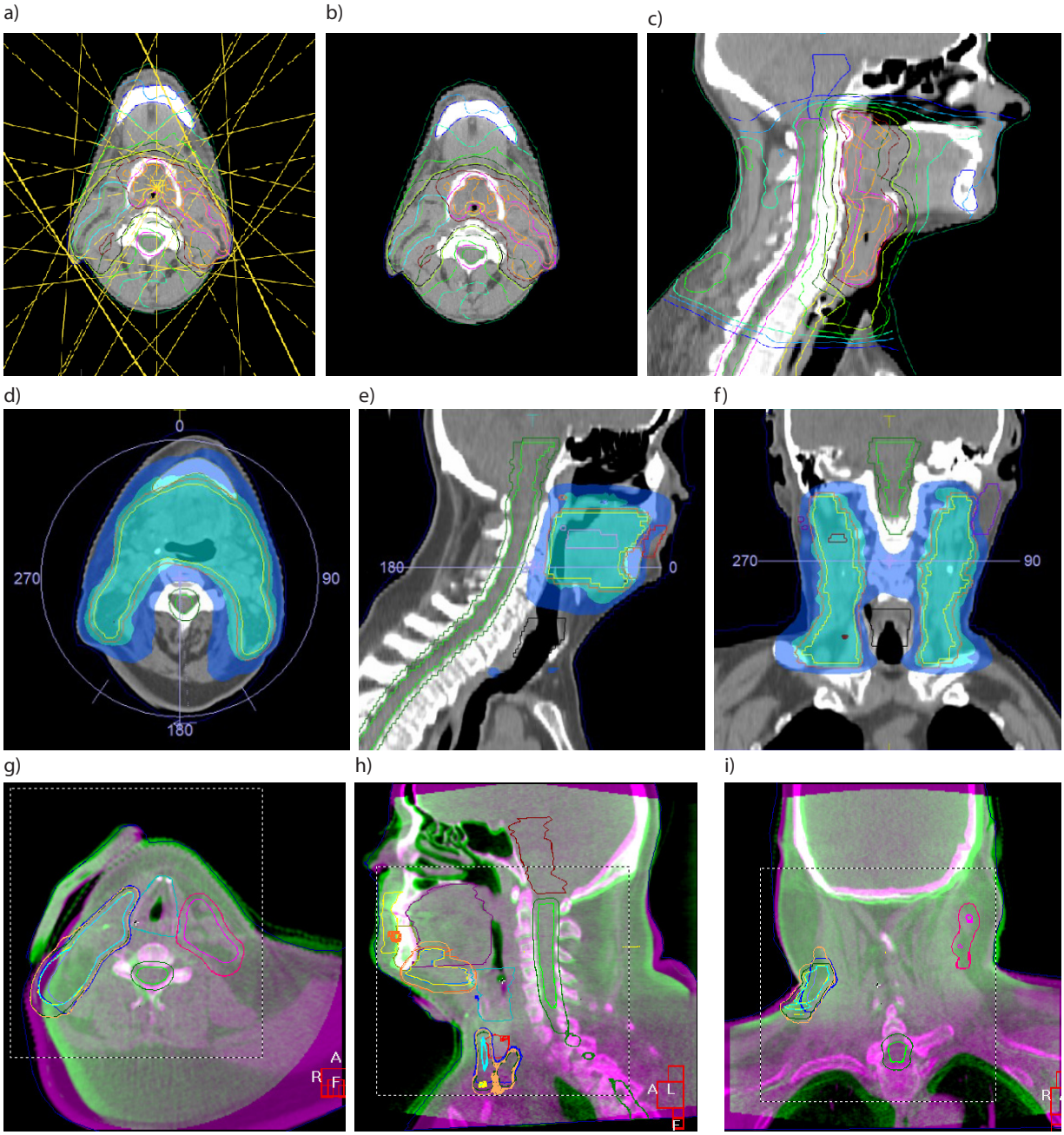

Figure 2. Use of computed tomography in radiotherapy planning and verification of the patient's positioning before starting radiotherapy. Radiotherapy planning with IMRT (intensity modulated radiotherapy): arrangement of radiation beams (**a**), distribution of radiation dose in the form of isodoses on the transverse cross-section (**b**) and sagittal cross-section (**c**). VMAT (volumetric modulated arc therapy) radiotherapy planning: distribution of the dose over the transverse (**d**), sagittal (**e**) and frontal (**f**) cross-sections. Verification of patient positioning by superimposing the location CT images (pink) and kV CBCT (cone beam computed tomography) made before irradiation (green) on the transverse (**g**), sagittal (**h**) and frontal (**i**) cross-section. The computer system reads shifts along the x, y, z axes and then corrects the position of the patient

Performing a CT scan was also one of the recommendations during the follow-up of HNC patients. According to the algorithm of NCCN (National Comprehensive Cancer Network), as well as the Polish and European guidelines — the CT examination of the head and neck region should be performed not earlier than 6 months after the end of treatment and also not more often than every 6 months. NCCN's recommendations also suggest that patients after HNC treatment should have a chest CT because of the increased risk of lung cancer, especially in smokers [14, 46, 47].

RECIST criteria (response evaluation criteria in solid tumors), are used to assess the response to chemotherapy and *ir*-RECIST *(immune-related* RECIST) for immunotherapy. These criteria are based on a comparison of the size and number of neoplastic lesions measured in the initial and control — after treatment — CT [48]. A study by Kim et al. [49] which

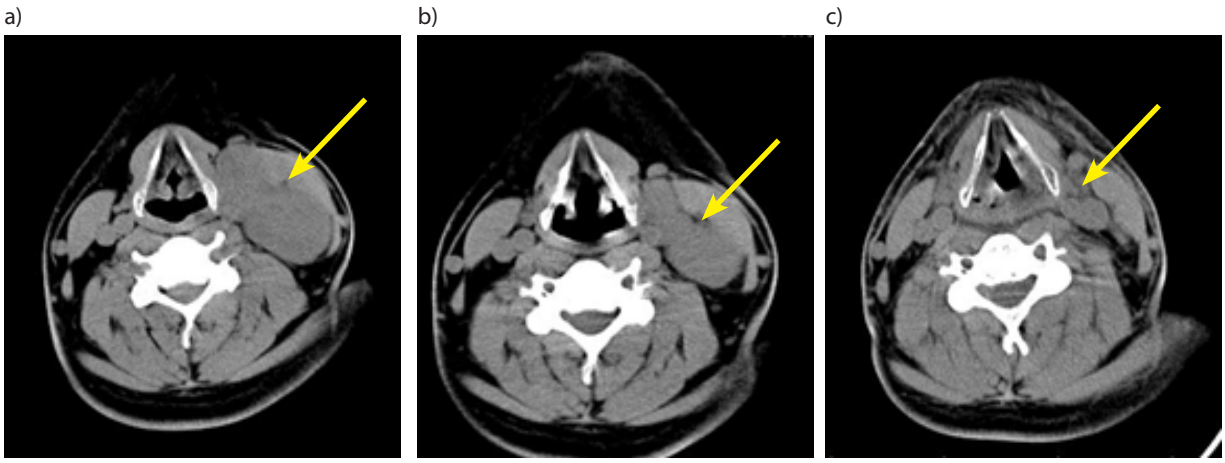

Figure 3. Use of computed tomography (CT) to evaluate the results of combined therapy. A male patient with squamous cell carcinoma of the tonsil, in clinical stage of T2N3M0. (**a**) CT of the neck region before treatment — a visible bulky lymph nodes of group III cervical nodes on the right (arrow). (**b**) after induction chemotherapy (3 courses of TPF). (**c**) a follow-up exam after radical MV IMRT (intensity modulated radiotherapy) up to the total dose of 70 Gy in 35 fractions with simultaneous chemotherapy with weekly cisplatin at 40 mg/m^2

compares methods of diagnostics of local/regional HNC recurrences, shows that the sensitivity and specificity of CT in this aspect is: 89.9% vs 85.7%, respectively.

Magnetic resonance

Magnetic resonance (MR) is an imaging method of choice for the head and neck region diagnostics [2]. It does not use ionizing radiation, so in this regard it is a safer method than CT. The basis of the MR method is the phenomenon of nuclear magnetic resonance, consisting in excitation of nuclei of hydrogen atoms in tissues located in an external magnetic field, through rapid changes in this field. The electromagnetic radiation caused by the system's return to equilibrium is recorded and processed by computer systems.

The diagnostic accuracy of the MR is influenced, among others, by the magnitude of the magnetic field strength expressed in tesla (T). The higher the T number, the better the contrast between the different structures, which is particularly important in the assessment of tissues and organs in the head and neck region, where a large number of small adjacent structures such as nerves, vessels and lymph nodes are present. Currently, 1.5T and 3T devices are standard equipment of radiology departments, while 7T systems are at the experimental testing phase [50, 51]. The MR examination includes various options — sequences that can be performed in a single session on this diagnostic equipment. Each subsequent sequence prolongs the examination time by 2–10 minutes, during which the patient must remain motionless in one position, which may be a problem, for example, for patients with bone and joint pain [2, 8]. However, individual MR sequences offer new possibilities to differentiate between benign and malignant lesions. The standard sequences in the MR examination are: T1-weighted scan — shows individual anatomical structures in excellent resolution, T2-weighted scan — shows edema and related pathologies. STIR (short TI inversion recovery), on the other hand, eliminates disturbances originating from adipose tissue [8]. Newer sequences, now widely studied, are DWI (diffusion-weighted imaging) and ADC (apparent diffusion coefficient). The DWI sequence shows diffusion, i.e. movements of water molecules in the extracellular space, reveals the structure of the tumor and depends on the density of cells in a given tissue. Reduction of diffusion gives a high DWI signal (hyperintense foci, "lighter" spots), which is used to characterize and evaluate the extent of cancer infiltration. Changes that resemble edema, fibrosis, inflammation decrease the DWI signal (hypointense, "darker" foci). However, sometimes there are deviations from this rule: tumor necrosis decreases the DWI signal, which can make it difficult to estimate the size of the tumor, while non-malignant ulceration increases the DWI signal suggesting its neoplastic origin. Also some normal tissues, i.e. lymphatic tissue and salivary glands are characterized by an increased DWI signal, so this sequence becomes less useful in the diagnosis of metastases to lymph nodes. The ADC sequence is used to diagnose and describe primary lesions, but above all, to monitor responses to non-operative treatment, i.e. radio- or chemotherapy (CT). It allows to distinguish local recurrences from inflammatory lesions or fibrosis after RT, which gives an advantage over PET scans, which do not always allow for such differentiation [2]. Currently, the predictive value of the ADC sequence is subject to verification in clinical trials. Preliminary studies show that the increased ADC in the tumor before treatment — associated with the presence of necrosis, low cell density and a high component of stroma in tissue — correlates with a higher cancer resistance to radiochemotherapy (RCT) [52].

The cross-sections obtained from MR are characterized by very good imaging of soft tissues due to high contrast between individual structures [2, 8, 53]. MR can be used to

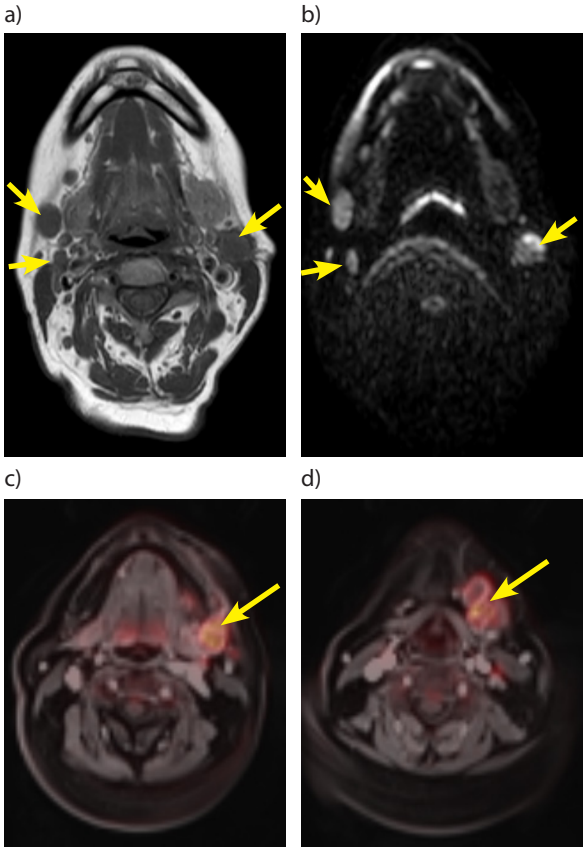

Figure 4. Image of metastatic lymph nodes (arrows) in sequence (**a**) T1- weighted TSE (turbo spin echo), (**b**) DWI (diffusion-weighted imaging) and (**c, d**) PET/MR. (**a, b**) A female patient with T2N2cM0 squamous cell carcinoma of the tonsil with bilateral metastases to cervical lymph nodes of group II. (**c, d**) A female patient with T3N2bM0 squamous cell carcinoma of the left buccal mucosa with metastatic lymph nodes in group II (**c**) metastatic bulky lymph nodes (**d**) in group III on the right side (arrow)

accurately visualize the boundaries of the tumor and the infiltration of adjacent structures. This study is particularly well suited for the diagnosis of perineural infiltration [2, 53]. However, MR examination has limitations — it is characterized by poorer quality of bone structure imaging. Therefore, in the case of infiltration of e.g. skull base structures, the CT is an examination of choice, which visualizes bones much better than MR[54]. The specificity of MR, determined in a meta-analysis by Sun et al. in relation to the diagnosis of metastatic lymph nodes in HNC, is significantly higher than CT (81% vs 72%), with lower sensitivity of MR in this regard (80% vs 84%). In diagnostics of HNC distant metastases, MR is particularly useful in imaging lesions in the brain. T1- and T2-weighted sequences are routinely performed, as well as the pathological contrast enhancement evaluation in order to determine the structure of the tumor. The FLAIR sequence, on the other hand, provides an excellent contrast between metastatic lesion and nerve tissue [50, 55]. In addition, for the diagnosis of hepatic metastases, the T1- and T2-weighted sequences, the DWI sequence and the use of an intravenous contrast agent provide accurate imaging of lesions with varying degrees of vascularity [56]. In the diagnosis of liver tumors, MR and CT examinations show similar sensitivity, with a slight predominance of MR [55].

Magnetic resonance spectroscopy (MRS) allows for the analysis of the concentration of metabolites in tissues exposed to electromagnetic radiation. One of the more common MRS techniques used in HNC assessment is the proton MRS (1H-MRS), which detects increased choline metabolites (Cho) in tumor tissues, reflecting cell proliferation and changes in cell membrane. Elevated Cho/creatine (Cr) ratio is characteristic for squamous cell HNC. Regions of hypoxia and necrosis in tumors are described by the peak of lipids and lactates in the spectroscopic analysis [56].

During the MR examination it is possible to use an intravenous contrast agent, based mostly on chelated gadolinium compounds. In some cases tissue-specific contrast agents can be used, e.g. in the diagnosis of hepatic metastatic lesions, these will be the agents containing iron oxide molecules showing affinity to the reticuloendothelial system and hepatocytes [13, 57]. Until recently, these media, in contrast to those used during CT, were considered to be completely safe, also for patients with renal diseases. However, studies have shown an increasing incidence of nephrotoxicity and nephrogenic systemic fibrosis (NSF) after gadoline-based agent administration, and the risk of these complications increases with deteriorated renal function [58]. Another contraindication for MR scan is the presence of metal elements in the patient's body (cardiac pacemakers, cochlear implants, intrauterine contraceptive devices, metal shavings in an eyeball, surgical clips, metal surgical stitches), which is caused by the use of high intensity magnetic field during the examination. Although the latest stimulation devices (cardiostimulators, etc.) are already manufactured from alloys that are not contraindications for MR scanning, they are nevertheless a source of image-distorting artifacts [59].

In addition to its obvious role in the initial imaging diagnostics of patients with HNC, MR is used in the treatment planning process — RT — of both primary tumors and distant metastases (e.g. CNS). The new generation of devices dedicated to teleradiotherapy are combinations of MR with a linear accelerator or a device containing a source of cobalt-60. Such hybrids allow, among others, to obtain a high contrast of soft tissues, no exposure to X-rays, or no need to implant markers in order to position the patient on the therapeutic device [60]. Although RT planning is currently still based on the CT scan, new programs and algorithms compatible with modern hybrid devices are being developed, allowing RT to be planned directly from MR scans, which would increase the precision of treatment [2, 59]. However, the standard of conduct, among others in RT changes in the CNS, is the determination of areas to RT based on the fusion of the basic CT scan with a diagnostic MR examination or MR performed in a therapeutic position,

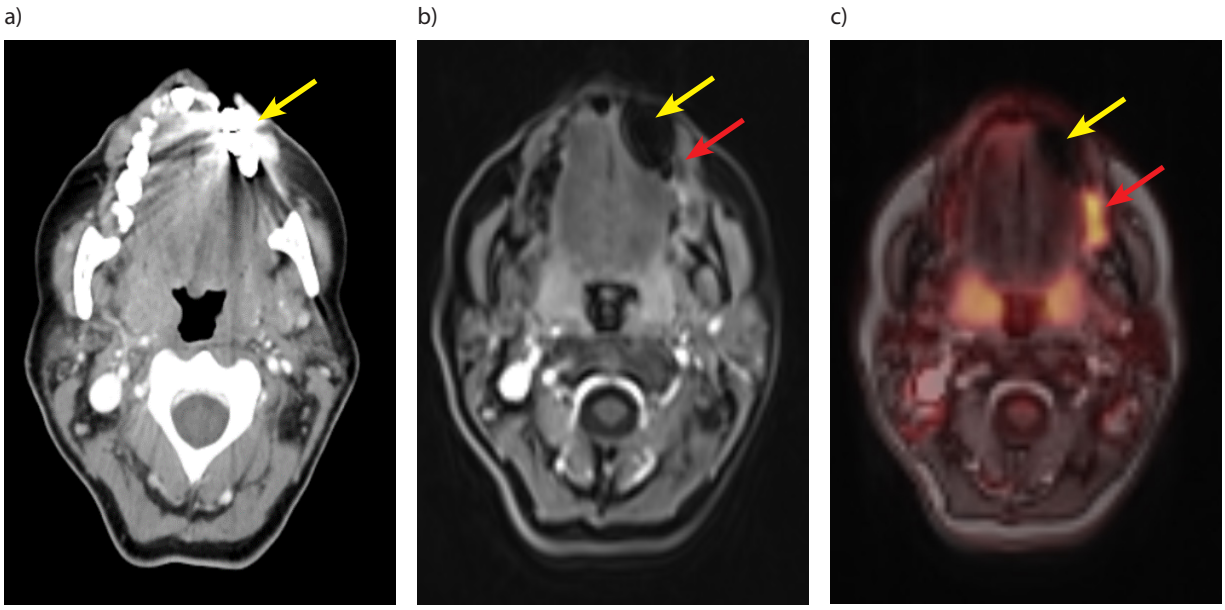

Figure 5. An artifact in imaging examinations. An artifact (yellow arrows) from amalgam tooth fillings in the CT (**a**), MR (**b**) and PET/MR (**c**) images, making it difficult to diagnose lower gingiva lesions on the left side (red arrows)

so far (still, few centers have a special "attachment" to the MR device serving this purpose) [61].

According to the recommendations of NCCN [47], MR may be used as a follow-up examination after the end of treatment of patients with HNC according to the following scheme: first MR imaging after 6 months from the end of treatment, another at intervals of 6 months or in case of recurrence suspicion. MR in comparison with CT seems to be a follow-up examination of choice, mainly due to the greater possibility of visualization of small anatomical structures in soft tissues and differentiation between the lesions after RT and the local recurrence. Only in case of suspicion of bone structure infiltration the diagnosis should be additionally deepened by CT scan [54]. The sensitivity and specificity of MR as a follow-up examination, especially when using the DWI sequence, is high — over 90% [62].

However, not all centers have MR equipment at their disposal due to high costs of equipment purchase. CT is relatively cheaper and thus more widely used in clinical practice compared to MR [63].

Angiography

Angiography is an invasive method of blood vessel examination, which consists in injecting a contrast agent into the vessel and registering a series of X-ray images. It allows to differentiate tumors of vascular origin from solid tumors and to visualize places of bleeding. In the case of tumors with properly depicted vascular system, this examination can be combined with endovascular obliteration [64]. HNC are the main causes of difficult to control hemorrhages — spontaneous, as well as complications of oncological treatment. Diagnostic angiography with vascular contrast is a key examination in such cases. A presence of angiographic catheter enables embolization of the pathologically changed vessel, which effectively prevents life-threatening hemorrhages [65].

Currently, the role of non-invasive methods, such as computed tomographic angiography (angio-CT), is increasing. It is a method of vessel imaging with the use of spiral CT after intravenous contrast administration [66]. This method is used for mapping of blood vessels of the limb and their evaluation before the collection of the skin flap for transplantation, as part of reconstruction operations of defects resulting from surgical treatment of patients with HNC. Appropriate diagnostics of skin graft vascularity prevents rejection of the transplant due to local blood circulation insufficiency and allows to maintain effective vascularity of the limb from which the graft was taken [67, 68].

Similarly, magnetic resonance angiography (MRA) is also used. The quality of vascular imaging in both methods is similar. It is possible to perform both of these examinations using the *whole-body* technique, which allows for the assessment of vascularity at the place where the skin graft is collected and at the target transplant site [69].

Positron emission tomography (PET)

PET scan is a method of molecular imaging of tissues, increasingly used in the diagnosis of cancer. The basis of this technique is the phenomenon of annihilation of positron--electron pair, as a result of which high-energy photons are created. The positrons are derived from the radioactive decay of a radiopharmaceutical component administered

to the patient. The source of electrons are tissues and body fluids of the patient. The radiopharmaceutical component accumulates in characteristic tissues, and the spatial distribution of photon emission is the initial image of the study. 90–95% of PET tests are performed with deoxyglucose radiolabeled with fluorine 18 (^{18}F-FDG). This compound is transported to the cell in the same way as glucose and, just as glucose, is subjected to glycolysis processes until the phosphorylation reaction, the products of which are then deposited in the cell [2, 70]. The phenomenon of increased glucose uptake and metabolism compared to normal tissues is characteristic for most types of cancer [70]. It also occurs in: inflammation, edema, infection, pre-cancerous lesions, healing postoperative lesions, directly after the effort in skeletal muscles and physiologically in the brain tissue. The above mentioned changes in glucose uptake may lead to false positive diagnoses, on the other hand, increased glucose metabolism in muscles or brain tissue may form a background hindering the proper diagnosis of the tumor [2, 8]. Anderson et al. [70] demonstrated the possibility of distinguishing ^{18}F-FDG uptake caused by inflammation from the one caused by cancer. These cases differ in the uptake kinetics of ^{18}F-FDG: during the examination, in 60–120 minutes after administering the radiopharmaceutical substance, a decrease was observed in ^{18}F-FDG accumulation in the inflammatory site, while ^{18}F-FDG metabolism was still increasing in the tumor tissue. On the other hand, e.g. necrosis in a neoplastic tumor, high blood glucose and insulin levels affect false negative results [2].

Although ^{18}F-FDG is a commonly used radiopharmaceutical substance in PET studies, PET imaging also uses alternative radiotracers — not only in experimental studies, but more and more often in clinical practice. One of them is ^{18}F-fluoromisonidazole (FMISO), which in the case of HNC allows for illustrate the foci of hypoxia and perfusion in tissues [71]. These factors have a predictive value in the treatment of HNC patients — hypoxia in the tumor area has a negative impact on RT treatment results [72]. FMISO belongs to the group of nitroimidazoles — chemical compounds which were developed as early as in the 1970s as markers of cell hypoxia and were used as "radiosensitizers" — substances increasing the sensitivity of cells for ionizing radiation [73]. Nitroimidazoles in hypoxic cells are reduced to form of a reactive intermediate compound. Under normal conditions these molecules are re-oxidized to the parent compound and diffuse from the cell. However, hypoxia causes further reduction and the compound is irreversibly trapped in the cell. These reactions occur at a rate that is inversely proportional to the oxygen pressure in the cell. Since the reduction of nitroimidazoles requires the presence of active tissue reductases, these compounds accumulate in living, oxygenated cells, but are not found in cells undergoing apoptosis or necrosis [74].

Promising results of clinical studies on HNC hypoxia imaging are also associated with another nitroimidazole — ^{18}F-fluoroazomycinarabinozide (^{18}F-FAZA), but its clinical usefulness must be confirmed in further studies [75]. Other radiotracers are in the experimental stage, i.e.: ^{18}F-FETNIM (^{18}F-fluoroerythronitroimidazole), ^{18}F-EF5 (^{18}F-2-(2-Nitro-1-H-imidazol-1-yl)-N-(2,2,3,3,3-pentafluoropropyl)acetamide) and Cu-ATSM (Cu-diacetl-bis (^{4}N-methylthiosemicarbazone)) — hypoxia markers, ^{18}F-FET (^{18}F-fluoroethyl-L-tyrosine) — selectively accumulated in cells of squamous cell HNC and allowing for differentiation of inflammatory reaction from cancer and ^{11}C-choline (CHOL) — accumulated in malignant tumors similarly to ^{18}F-FDG, but to a lesser extent in muscles, which eliminates background artifacts hindering diagnostics [74, 76–78]. The problem with the use of alternative radiopharmaceuticals is the short half-life period of these compounds. This results in the given centre's need to have a cyclotron for the production of such radiotracers. It entails significant costs, which means that only few centers can perform PET scans with substances other than ^{18}F-FDG [79].

Positron emission tomography/Computed tomography (PET/CT)

The enrichment of functional PET imaging with CT fusion increases the precision of the method through better anatomical mapping, allowing for more accurate localization and evaluation of the morphology of metabolic variations [80]. The CT scan performed within PET/CT is a low-dose X-ray examination without intravenous contrast agent. It is not a fully diagnostic examination. Its aim is to facilitate anatomical localization of foci of increased glucose uptake [81]. Therefore, PET/CT is rarely used to evaluate the tumor because of the weak tissue contrast obtained in CT scans without intravenous contrast agent. Insufficient detection of small tumors, not exceeding 5 mm, is also an imperfection of the examination. Compared to other imaging methods, it is more accurate in detecting metastatic lymph nodes. The sensitivity and specificity of PET/CT in the determination of the N parameter (according to TNM) is 80% and 86%, respectively. It is also possible to visualize eventual distant metastases or a synchronous tumor during a single examination, due to the fact that the entire patient's body is included in the PET/CT scan [2]. This method is also applicable for detecting a primary tumor in the case of lymph node metastases from an unknown primary [2, 8]. Such cases constitute 2–7% of all HNCs. In 25–54% of them a primary tumor is identified by PET/CT scan. However, the most important role of PET/CT in the imaging diagnostics of the head and neck region is to monitor the effects of treatment after radical RCT. In order to prevent false positives, PET/CT should be carried out no earlier than 3 months after the end of treatment [2, 82]. The sensitivity and specificity of PET/CT in the determination of possible residual lesion/recurrence is 94% and 82%, respectively [2]. A negative

PET/CT scan 12 weeks after the end of RCT is currently the best positive prognostic factor [83]. The PET/CT examination is characterized by a high negative prediction value [82]. It helps to prevent unnecessary surgeries after an earlier RCT, which increase mortality rate among this group of patients. For economic reasons, this examination is also a cost-effective tool to control the effects of treatment [2, 83].

Modern RT techniques allow to administer a sufficiently high dose of ionizing radiation to the tumor area with maximum healthy tissue sparing. Therefore, irradiation volumes must be precisely defined and one of useful examinations in this respect is PET/CT. The detection of pathological foci of increased ^{18}F-FDG uptake in lymph nodes of normal size allows to covered them with an appropriately high dose of ionizing radiation — thus increasing the probability of radical treatment. On the other hand, PET/CT may reveal necrotic lesions in the tumor, which will result in a smaller target volume and decrease volume of healthy tissue in the irradiated area. The main problem with the use of PET/CT in the definition of RT volumes is the determination of the cut-off point of the ^{18}F-FDG uptake (SUV — standardized uptake value). This may lead to overestimation or underestimation of the volume of neoplastic lesions [84]. Some researchers contoured the areas on the basis of 50% of the maximum intensity of ^{18}F-FDG uptake by the tumor [85]. Others considered ^{18}F-FDG uptake by liver tissue uptake as the limit value [86]. Wang et al. [87] investigated the SUV value above 2.5 as the basis for contouring the target volumes. Despite the lack of consensus on this issue, the vast majority of researchers demonstrated a positive effect of the PET/CT on the precision of the determination of the irradiation volume [84].

Positron emission tomography/Magnetic resonance (PET/MR)

A hybrid of PET and MR is a modern combination of high quality anatomical MR and functional and metabolic

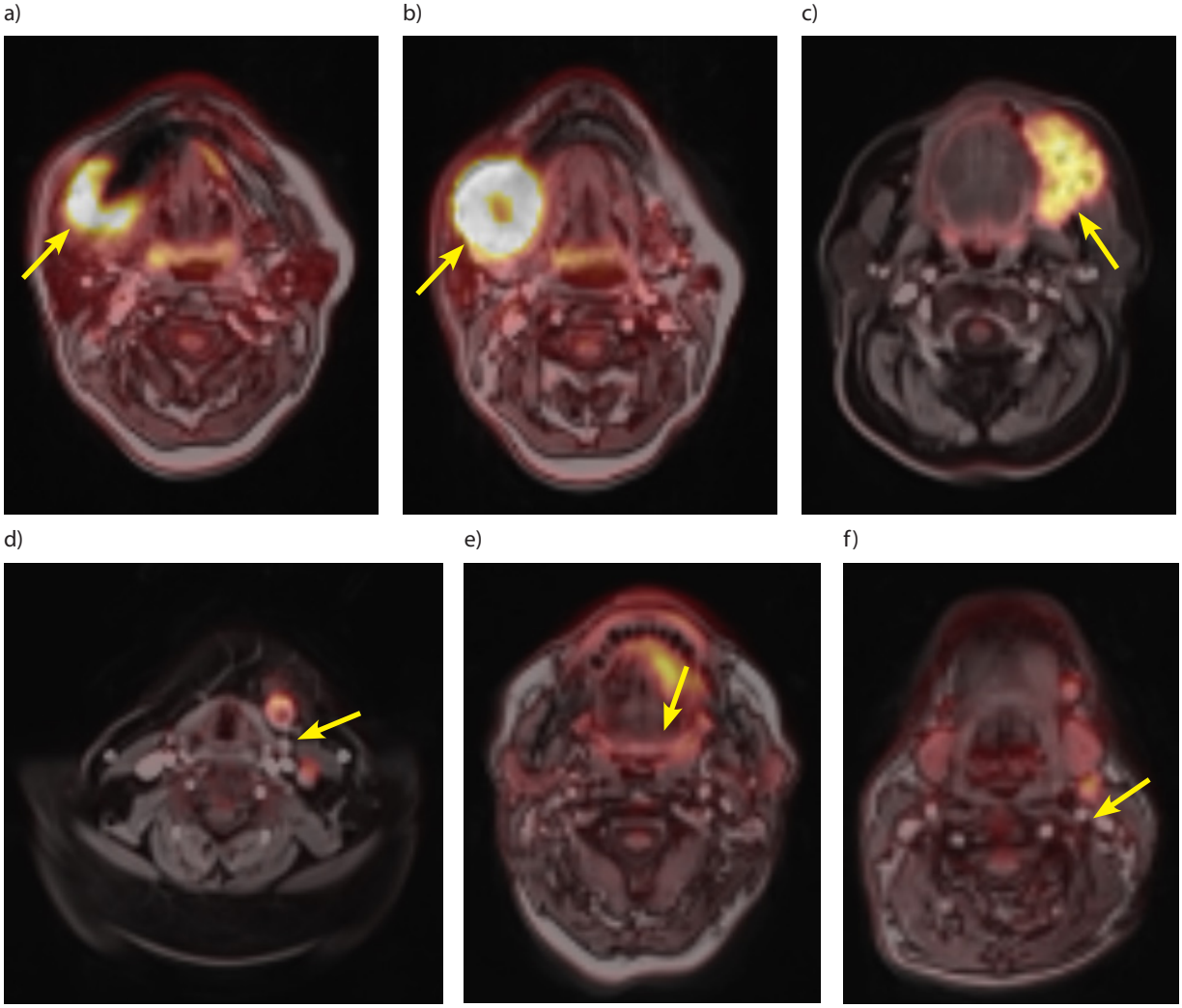

Figure 6. Use of PET/MR in diagnostics of the head and neck region tumors. (**a**, **b**) A female patient with diagnosed keratinized squamous cell carcinoma of the right submandibular salivary gland (arrow) at T3N0M0 clinical stage. (**c**, **d**) A female patient with squamous cell carcinoma of the left buccal mucosa (**c**) at T3N2bM0 clinical stage, (**d**) a metastatic cervical lymph node at the borderline of left III and IV groups. (**e**, **f**) Patient with diagnosis of squamous cell carcinoma the floor of the mouth at T1N2cM0 clinical stage (**e**), a metastatic lymph node of left group II of cervical lymph nodes (**f**)

imaging obtained from PET using most often ^{18}F-FDG [88]. There are only several studies that have evaluated the clinical benefit of such a combination in the diagnosis of patients with HNC, so far. PET/MR seems to have an advantage over PET/CT, among others, due to the possibility of obtaining simultaneously high contrast in soft tissues and fewer artifacts derived from implants and dental fillings [87, 88]. The use of low-dose CT in PET/CT speaks in favor of PET/MR imaging [89]. Another advantage of PET/MR hybrid is the possibility of using individual sequences of fully diagnostic MR, such as DWI sequence, T1- and T2- weighted sequence [90, 91]. The sensitivity and specificity of the PET/MR in HNC diagnostics has not yet been determined, but on the basis of preliminary studies it seems to be particularly useful in the imaging of metastatic lymph nodes and in case of suspicion of recurrence after radical treatment. The promising results also concern the use of PET/MR hybrids in the diagnosis of HNC distant metastases into the liver and brain and as a basis for planning areas for radiotherapy [88–90].

Scintigraphy

As mentioned earlier, the skeletal system is the second most frequent location of HNC metastases [11]. Scintigraphic scan is a standard procedure in the diagnosis of bone metastases. It is one of the longest used techniques of nuclear medicine, whose principle of operation is similar to PET scans. A patient receives an intravenous radiotracer and then the whole body is scanned using a gamma camera. Unlike PET, the image obtained during scintigraphy is a projection of the bone system in one plane [91, 92]. A scan with radiotracers consisting of diphosphates radiolabeled with technetium-99 (^{99}Tc) has a high sensitivity (> 90%) to detect changes in bones. However, studies [91, 93, 94] have shown that in the diagnosis of bone metastases PET/CT is characterized by higher precision in the localization of bone lesions, as well as higher sensitivity and specificity than scintigraphy, especially when the radiotracer in PET/CT is [^{18}F]-NaF (sodium fluoride radiolabeled with 18-fluoride).

Scintigraphy is also used in the assessment of salivary gland function in connection with planned radiotherapy treatment in HNC. RT in the head and neck region often causes xerostomia as a result of salivary gland damage and secretive function disorders. Therefore an attempt to protect salivary glands as risk organs during the RT planning. Scintigraphy is performed after administration of ^{99}Tc, and the image of the salivary glands suggests which gland or area of the gland is the most secretively active. This helps to determine which areas should be particularly protected during RT planning [95, 96].

Summary

Anatomical and metabolic imaging methods differ in sensitivity, specificity and diagnostic accuracy. Information obtained thanks to them supports making the right therapeutic decision, precise implementation of medical procedures (e.g. diagnostics, radiotherapy) and monitoring of treatment results. Each of these methods has its strengths and weaknesses in HNC imaging, so the choice of therapy should not be made on the basis of a single imaging examination.

Abbreviations

ADC — apparent diffusion coefficient
CBCT — cone beam computed tomography, kilovolt conical computed tomography
CHOL — choline radiolabeled with carbon-11
CR — computed radiography
Cu-ATSM — Cu-diacetl-bis (N^4-methylthiosemicarbazone)
DR — digital radiography
DWI — diffusion-weighted imaging
EPID — electronic portal imaging device
FDA — Food and Drug Administration
^{18}F-EF5 — 2-(2-Nitro-1-H-imidazol-1-yl)-N-(2,2,3,3,3-pentafluoropropyl)acetamide radiolabeled with fluorine-18
^{18}F-FAZA — azomycinarabinoside radiolabeled with fluorine-18
^{18}F-FDG — deoxyglucose radiolabeled with fluorine-18
^{18}F-FET — ethyl-L-tyrosine radiolabeled with fluorine-18
^{18}F-FETNIM — erythronitroimidazole radiolabeled with fluorine-18
FMISO — misonidazoleradiolabeled with fluorine-18
HNC — head and neck cancers
IGRT— image-guided radiation therapy, image-controlled radiotherapy
IMRT — intensity modulated radiotherapy
IOUS — intraoral ultrasonography
ir-RECIST — immune-related response evaluation criteria in solid tumors
NSF — nephrogenic systemic fibrosis
RCT — radiotherapy and chemotherapy
RECIST — response evaluation criteria in solid tumors
RT— radiotherapy
SBRT — stereotactic body radiotherapy
STIR — short TI inversion recovery
SUV — standardized uptake value
TSE — turbo spin echo
VMAT — volumetric modulated arc therapy

Conflict of interest: none declared

Ewa Sierko, MD, PhD
Medical University of Bialystok
Department of Oncology
ul. Ogrodowa 12
15–025 Białystok, Poland
e-mail: ewa.sierko@iq.pl

Received: 19 Jul 2018
Accepted: 24 Sept 2018

References

1. Wojciechowska U, Didkowska J. Zachorowania i zgony na nowotwory złośliwe w Polsce. Warszawa: Centrum Onkologii — Instytut im. Marii Skłodowskiej-Curie, Krajowy Rejestr Nowotworów. (http: //onkologia.org.pl/raporty/; cited 23 Jun 2018).
2. Burkill GJ, Evans RM, Ramman VV et al. Modern radiology in the management of head and neck cancer. *Clin Oncol* (*R Coll Radiol*) 2016; 28: 440–450.
3. Batko T, Kosiak W. Zastosowanie badań ultrasonograficznych węzłów chłonnych u dzieci i młodzieży w gabinecie lekarza rodzinnego i pediatry — na podstawie doświadczeń własnych. *Dev Period Med* 2013; (2): 137–142.
4. Kallalli B, Rawson K, Kumari V et al. Comparison between clinical examination, ultrasonography and computed tomography in assessment of cervical lymph node metastasis in oral squamous cell carcinoma. *J Indian Acad Oral Med Radiol* 2016; 28: 364–369.
5. Sureshkannan P, Vijayprabhu JR. Role of ultrasound in detection of metastatic neck nodes in patients with oral cancer. *Indian J Dent Res* 2011; 22: 419–423.
6. Geetha N, Hallur N, Goudar G et al. Cervical lymph node metastasis in oral squamous carcinoma preoperative assessment and histopathology after neck dissection. *J Maxillofac Oral Surg* 2010; 9: 42–47.
7. Saafan ME, Elguindy AS, Abdel-Aziz MF et al. Assessment of cervical lymph nodes in squamous cell carcinoma of the head and neck. *Surgery Curr Res* 2013; 3: 145. doi.: 10.4172/2161-1076.1000145.
8. Lewis-Jones H, Colley S, Gibson D. Imaging in head and neck cancer: United Kingdom National Multidisciplinary Guidelines. J *Laryngol Otol* 2016; 130(S2): S28–S31.
9. Shetty D, Jayade BV, Joshi SK et al. Accuracy of palpation, ultrasonography and computed tomography in the evaluation of metastatic cervical lymph nodes in head and neck cancer. *Indian J Dent* 2015; 6: 121–124.
10. Chammas M, Macedo A, Moyses A et al. Relationship between the appearance of tongue carcinoma on intraoral ultrasonography and neck metastasis. *Oral Radiol* 2011; 27: 1–7.
11. Ferlito A, Shaha AR, Silver EC et al. Incidence and sites of distant metastases from head and neck cancer. *ORL J Otorhinolaryngol Relat Spec* 2001; 63: 202–207.
12. Gierbliński I, Wocial T. Ultrasonografia z kontrastem w diagnostyce zmian ogniskowych w wątrobie. *Nowotwory J Oncol* 2007; 57: 37–46.
13. Kowalski H. Podstawy teoretyczne badań obrazowych. In: *Radiologia: diagnostyka obrazowa: Rtg, TK, USG, MR i radioizotopy*. Pruszyński B (ed.). Warszawa: Wydawnictwo Lekarskie PZWL, 2005: 21–64.
14. Kawecki A. Nowotwory narządów głowy i szyi. In: *Onkologia kliniczna.* Krzakowski M. Potemski P, Warzocha K et al (eds.). Gdańsk: Via Medica, 2015: 493–522.
15. Wierzbicka M, Popko M, Piskadło K et al. Comparison of positron emission tomography/computed tomography imaging and ultrasound in surveillance of head and neck cancer — The 3-year experience of the ENT Department in Poznań. *Rep Pract Oncol Radiother* 2011; 16: 184–188.
16. Franzone P, Fiorentino A, Barra S et al. Image-guided radiation therapy (IGRT): practical recommendations of Italian Association of Radiation Oncology (AIRO). *Radiol Med* 2016; 121: 958–965.
17. Fontanarosa D, van der Meer S, Bamber J et al. Review of ultrasound image guidance in external beam radiotherapy: I. Treatment planning and inter-fraction motion management. *Phys Med Biol* 2015; 60: R77–114.
18. O'Shea T, Bamber J, Fontanarosa D et al. Review of ultrasound image guidance in external beam radiotherapy part II: intra-fraction motion management and novel applications. *Phys Med Biol* 2016; 61: R90–137.
19. Wolny T, Linek P. Wprowadzenie do diagnostyki obrazowej narządu ruchu dla fizjoterapeutów. *Rehab Prakt* 2016; (1): 22–28.
20. Mackiewicz S. Detektory promieniowania stosowane w cyfrowej radiografii bezpośredniej. *Badania Nieniszczące i Diagnostyka* 2017; 2: 44–51.
21. Jassem J, Kawecki A. Nowotwory nabłonkowe narządów głowy i szyi. Zalecenia diagnostyczno-terapeutyczne Polskiej Unii Onkologii. *Nowotwory J Oncol* 2003; 53: 552–569.
22. Petkowicz B, Banakiewicz K, Zieliński P et al. Powikłania występujące w jamie ustnej w następstwie radioterapii. *Gastroenterol Pol* 2012; 19: 60–63.
23. Piekoszewska-Ziętek P, Turska-Szybka A, Olczak-Kowalczyk D. Odontogenic infections — review of the literature. *Nowa Stomatol* 2016; 21: 120–134.
24. Wójcik G, Szulc A, Stawińska T. Sinusitis in the context of diagnostics imaging. *J Educ Health Sport* 2016; 6: 63–72.
25. Ladd LM, Roth TD. Computed tomography and magnetic resonance imaging of bone tumors. *Semin Roentgenol* 2017; 52: 209–226.
26. Solis F, Gonzalez C. Raindrop skull. *N Engl J Med* 2018; 378: 1930–1930.
27. Bitelman VM, Lopez JA, Noqueira AB et al. "Punched out" multiple myeloma lytic lesions in the skull. *Autops Case Rep* 2016; 6: 7–9.
28. Warner GC, Cox GJ. Evaluation of chest radiography versus chest computed tomography in screening for pulmonary malignancy in advanced head and neck cancer. *J Otolaryngol* 2003; 32: 107–109.
29. Piotrowski T. Wybrane zagadnienia dotyczące planowania leczenia w radioterapii. Pracownia Planowania Leczenia, Zakład Fizyki Medycznej, Wielkopolskie Centrum Onkologii. Poznań, 2005.(www.slideshare.net/tomasz.piotrowski).
30. Dąbrowski A, Kukułowicz P, Sadowska E. 51 Wyniki kontroli radioterapii techniką zdjęć portalowych dla pacjentek napromienianych techniką box. *Rep Pract Oncol Radiother* 1999; 4: 125–125.
31. Lewcio-Szczęsna K, Samołyk N, Hempel D et al. Assessment of patient positioning error for BrainLab thermoplastic mask system during stereotactic radiosurgery of brain tumors. *Onkol Radioter* 2017: 42: 23–30.
32. Mijnheer B. EPID-based dosimetry and its relation to other 2D and 3D dose measurement techniques in radiation therapy. *J Phys Conf Ser* 2017; 847: 012024.
33. Allgower CE, Schreuder AN, Farr JB et al. Experiences with an application of industrial robotics for accurate patient positioning in proton radiotherapy. *Int J Med Robot* 2007; 3: 72–81.
34. Li J, Shi W, Andrews D. Comparison of online 6 degree-of-freedom image registration of varian TrueBeam cone-beam CT and BrainLab Exac Trac X-Ray for intracranial radiosurgery. *Technol Cancer Res Treat* 2017; 16: 339–343.
35. Ma J, Chang Z, Wang Z et al. Exac Trac X-ray 6 degree-of-freedom image-guidance for intracranial non-invasive stereotactic radiotherapy: comparison with kilo-voltage cone-beam CT. *Radiother Oncol* 2009; 93: 602–608.
36. Gevaert T, Verellen D, Engels B et al. Clinical evaluation of a robotic 6-degree of freedom treatment couch for frameless radiosurgery. *Int J Radiat Oncol Biol Phys* 2012; 83: 467–474.
37. Sun J, Li B, Li CJ et al. Computed tomography versus magnetic resonance imaging for diagnosing cervical lymph node metastasis of head and neck cancer: a systematic review and meta-analysis. *Onco Targets Ther* 2015; 8: 1291–1313.
38. Baxi AJ, Chintapalli K, Katkar A et al. Multimodality imaging findings in carcinoid tumors: a head-to-toe spectrum. *Radiographics* 2017; 37: 516–536.
39. Cho JK, Ow TJ, Lee AY et al. Preoperative 18F-FDG-PET/CT vs contrast-enhanced CT to identify regional nodal metastasis among patients with head and neck squamous cell carcinoma. *Otolaryngol Head Neck Surg* 2017; 157: 439–447.
40. Taghipour M, Mena E, Kruse MJ et al. Post-treatment 18F-FDG-PET/CT versus contrast-enhanced CT in patients with oropharyngeal squamous cell carcinoma: comparative effectiveness study. *Nucl Med Commun* 2017; 38: 250–258.
41. Rutkowski P, Zapaśnik A, Dębska-Ślizień A et al. Ostre uszkodzenie nerek po środkach kontrastowych — stanowisko Polskiego Towarzystwa Nefrologicznego. *Forum Nefrol* 2016; 9; 118–125.
42. U. S. Food and Drug Administration home page — Computed tomography — Information for healt care providers. https: //www.fda.gov/RadiationEmittingProducts/RadiationEmittingProductsandProcedures/MedicalImaging/MedicalX-Rays/ucm115317.htm (cited 24 Jun 2018).
43. Hansen C, Johansen J, Samsøe E et al. Consequences of introducing geometric GTV to CTV margin expansion in DAHANCA contouring guidelines for head and neck radiotherapy. *Radiother Oncol* 2018; 126: 43–47.
44. Konopka-Filippow M, Hempel D, Muśko A et al. Assessment of repositioning accuracy with X-ray volume imaging (XVI) verification of head and neck cancer patients during IMRT radiotherapy. *Onkol Radioter* 2015; 32: 37–47.
45. Jurkovic IA, Kocak-Uzel E, Mohamed ASR et al. Dosimetric and radiobiological evaluation of patient setup accuracy in head-and-neck radiotherapy using daily computed tomography-on-rails-based corrections. *J Med Phys* 2018; 43: 28–40.
46. Grégoire V, Lefebvre JL, Licitra L et al.; EHNS–ESMO–ESTRO Guidelines Working Group. Squamous cell carcinoma of the head and neck: EHNS–ESMO–ESTRO Clinical Practice Guidelines for diagnosis, treatment and follow-up. Ann Oncol 2010; 21 Suppl 5: v184–186.
47. National Comprehensive Cancer Network (NCCN) guidelines — head and neck cancers. 2.2018. https: //www.nccn.org/professionals/physician_gls/pdf/head-and-neck.pdf (cited 24 Jun 2018).
48. Le Lay J, Jarraya H, Lebellec L et al. irRECIST and iRECIST: the devil is in the details. *Ann Oncol* 2017; 28: 1676–1678.

49. Kim ES, Yoon DY, Moon JY et al. Detection of loco-regional recurrence in malignant head and neck tumors: a comparison of CT, MRI, and FDG PET-CT. *Acta Radiol* 2018 [Epub ahead of print].
50. Zwanenburg JJ, Hendrikse J, Visser F et al. Fluid attenuated inversion recovery (FLAIR) MRI at 7.0 Tesla: comparison with 1.5 and 3.0 Tesla. *Eur Radiol* 2010; 20: 915–922.
51. Moreno KF, Cornelius RS, Lucas FV et al. Using 3 Tesla magnetic resonance imaging in the pre-operative evaluation of tongue carcinoma. *J Laryngol Otol* 2017; 131: 793–800.
52. King AD, Thoeny HC. Functional MRI for the prediction of treatment response in head and neck squamous cell carcinoma: potential and limitations. *Cancer Imaging* 2016; 16: 23 doi.10.1186/s40644-016-0080-6.
53. Owecka M, Paprzycki W. Tomografia rezonansu magnetycznego nowotworów głowy i szyi. *Nowiny Lek* 2009; 78: 12–17.
54. Olmi P, Fallai C, Colagrande S et al. Staging and follow-up of nasopharyngeal carcinoma: magnetic resonance imaging versus computerized tomography. *Int J Radiat Oncol Biol Phys* 1995; 32: 795–800.
55. Cieszanowski A. The use of magnetic resonance imaging in oncology. *Onkol Prak Klin* 2013; 9: 60–69.
56. Dai YL, King AD. State of the art MRI in head and neck cancer. *Clin Radiol* 2018; 73: 45–59.
57. Shenoy-Bhangle A, Baliyan V, Kordbacheh H et al. Diffusion weighted magnetic resonance imaging of liver: Principles, clinical applications and recent updates. *World J Hepatol* 2017; 9: 1081–1091.
58. Witkowicz J. Czy stosowanie gadolinowych środków cieniujących u chorych z przewlekłą chorobą nerek jest bezpieczne? *Nephrol Dial Pol* 2009; 13: 10–14.
59. Brzeziński J, Zagrodzka M. Rezonans magnetyczny serca dla opornych — część 1. *Kardiol Dypl* 2009; 8: 84–89.
60. Skórska M. Nowe technologie wykorzystywane w procesie teleradioterapii w świetle doniesień zaprezentowanych podczas konferencji ASTRO 57 w San Antonio. *Lett Oncol Sci* 2016; 13: 24–29.
61. National Comprehensive Cancer Network (NCCN) guidelines. Central nervous system cancers. 1.2018. https: //www.nccn.org/professionals/physician_gls/pdf/cns.pdf (cited 24 Jun 2018).
62. Denaro N, Merlano MC, Russi EG. Follow-up in head and neck cancer: do more does it mean do better? A systematic review and our proposal based on our experience. *Clin Exp Otorhinolaryngol* 2016; 9: 287–297.
63. Tshering Vogel DW, Thoeny HC. Cross-sectional imaging in cancers of the head and neck: how we review and report. *Cancer Imaging* 2016; 16: 20. doi.10.1186/s40644-016-0075-3.
64. Wróbel M, Kopeć T, Juszkat R et al. Value of angiography and embolisation in treatment of head and neck vascular malformations at Otolaryngology Department, Poznań University of Medical Sciences, Poland. *Otolaryngol Pol* 2008; 62: 44–48.
65. Noy D, Rachmiel A, Emodi O et al. Transarterial embolization in maxillofacial intractable potentially life-threatening hemorrhage. *J Oral Maxillofac Surg* 2017; 75: 1223–1231.
66. Kowalewski K, Sąsiadek M. CT Angiography in diagnosing intracranial aneurysms. *Adv Clin Exp Med* 2004; 13: 349–358.
67. Tang T, Zhou P, Wang Z et al. Application of CT angiography in design of anterolateral thigh perforator flap for reconstruction of defect after head and neck cancer resection. *Zhonghua Er Bi Hou Tou Jing Wai Ke Za Zhi* 2015; 50: 383–387.
68. Chen SY, Lin WC, Deng SC et al. Assessment of the perforators of anterolateral thigh flaps using 64-section multidetector computed tomographic angiography in head and neck cancer reconstruction. *Eur J Surg Oncol* 2010; 36: 1004–1011.
69. Kramer M, Schwab SA, Nkenke E et al. Whole body magnetic resonance angiography and computed tomography angiography in the vascular mapping of head and neck: an intraindividual comparison. *Head Face Med* 2014; 10: 16. doi.10.1186/1746-160X-10–16.
70. Anderson CM, Chang T, Graham MM et al. Change of maximum standardized uptake value slope in dynamic triphasic [18F]-fluorodeoxyglucose positron emission tomography/computed tomography distinguishes malignancy from postradiation inflammation in head-and-neck squamous cell carcinoma: a prospective trial. *Int J Radiat Oncol Biol Phys* 2015; 91: 472–479.
71. Grkovski M, Schöder H, Lee NY et al. Multiparametric imaging of tumor hypoxia and perfusion with 18F-fluoromisonidazole dynamic PET in head and neck cancer. *J Nucl Med* 2017; 58: 1072–1080.
72. Martenka P, Roszak A. Niedotlenienie guza jako czynnik predykcyjny w radioterapii onkologicznej. *Ginekol Onkol* 2006; 4: 99–107.
73. Chapman JP. Hypoxic sensitisers — implications for radiation therapy. *N Engl J Med* 1979; 301: 1429–1432.
74. Fleming IN, Manavaki R, Blower PJ et al. Imaging tumour hypoxia with positron emission tomography. *Br J Cancer* 2014; 112: 238–250.
75. de Bruin L, Bollineni VR, Wachters JE et al. Assessment of hypoxic subvolumes in laryngeal cancer with 18F-fluoroazomycinarabinoside (18F-FAZA)-PET/CT scanning and immunohistochemistry. *Radiother Oncol* 2015; 117: 106–112.
76. Jiang J, Wu H, Huang M et al. Variability of gross tumor volume in nasopharyngeal carcinoma using 11C-choline and 18F-FDG PET/CT. *PloS One* 2015; 10: e0131801.doi.10.1371/journal.pone.0131801.
77. Haerle SK, Fischer DR, Schmid DT et al. 18 F-FET PET/CT in advanced head and neck squamous cell carcinoma: an intra-individual comparison with 18 F-FDG PET/CT. *Mol Imaging Biol* 2011; 13: 1036–1042.
78. Silvoniemi A, Suilamo S, Laitinen T et al. Repeatability of tumour hypoxia imaging using [^{18}F]EF5 PET/CT in head and neck cancer. *Eur J Nucl Med Mol Imaging* 2018; 45: 161–169.
79. Jones T, Price P. Development and experimental medicine applications of PET in oncology: a historical perspective. *Lancet Oncol* 2012; 13: e116–e125.
80. Szurowska E, Teodorczyk J, Dziadziuszko K et al. Pozytonowa tomografia emisyjna w onkologii z użyciem radiofarmaceutyków alternatywnych do 18F-fluorodeoksyglukozy. *Onkol Prakt Klin* 2013; 9: 197–199.
81. Boellaard R, O'Doherty MJ, Weber WA et al. FDG PET and PET/CT: EANM procedure guidelines for tumour PET imaging: version 1.0. *Eur J Nucl Med Mol Imaging* 2010; 37: 181–200.
82. Nelissen C, Sherriff J, Jones T et al. The role of positron emission tomography/computed tomography imaging in head and neck cancer after radical chemoradiotherapy: a single institution experience. *Clin Oncol (R Coll Radiol)* 2017; 29: 753–759.
83. Mehanna H, Wong WL, McConkey CC et al. PET-CT surveillance versus neck dissection in advanced head and neck cancer. *N Engl J Med* 2016; 374: 1444–1454.
84. Szyszko T, Cook G: PET/CT and PET/MRI in head and neck malignancy. *Clin Radiol* 2018; 73: 60–69.
85. Paulino AC, Johnstone PA. FDG-PET in radiotherapy treatment planning: Pandora's box? *Int J Radiat Oncol Biol Phys* 2004; 59: 4–5.
86. El-Bassiouni M, Ciernik IF, Davis JB et al. [18-FDG] PET-CT-based intensity-modulated radiotherapy treatment planning of head and neck cancer. *Int J Radiat Oncol Biol Phys* 2007; 69: 286–293.
87. Wang D, Schultz C, Jursinic PA et al. Initial experience of FDG-PET/CT guided IMRT of head-and neck carcinoma. *Int J Radiat Oncol Biol Phys* 2006; 65: 143–151.
88. Vitor T, Martins KM, Ionescu TM et al. PET/MRI: a novel hybrid imaging technique. Major clinical indications and preliminary experience in Brazil. *Einstein (São Paulo)* 2017; 15: 115–118.
89. Nakamoto Y, Tamai K, Saga T et al. Clinical value of image fusion from MR and PET in patients with head and neck cancer. *Mol Imaging Biol* 2009; 11: 46–53.
90. Rosenkrantz AB, Friedman K, Chandarana H et al. Current status of hybrid PET/MRI in oncologic imaging. *AJR Am J Roentgenol* 2016; 206: 162–172.
91. Al-Bulushi NK, Abouzied ME. Comparison of 18F-FDG PET/CT scan and 99mTc-MDP bone scintigraphy in detecting bone metastasis in head and neck tumors. *Nucl Med Commun* 2016; 37: 583–588.
92. Glaudemans AW, Signore A. Nuclear medicine imaging modalities: bone scintigraphy, PET-CT, SPECT-CT. In: *Bone metastases: A translational and clinical approach.* 2nd ed. Vassiliou V, Chow E, Kardamakis D (eds.). Dordrecht: Springer, 2014: 71–94.
93. Xu C, Zhang R, Zhang H et al. Comparison of 18FDG PET/PET-CT and bone scintigraphy for detecting bone metastases in patients with nasopharyngeal cancer: a meta-analysis. *Oncotarget* 2017; 8: 59740–59747.
94. Lopez R, Gantet P, Julian A et al. Value of PET/CT 3D visualization of head and neck squamous cell carcinoma extended to mandible. *J Craniomaxillofac Surg* 2018; 46: 743–748.
95. Loimu V, Seppälä T, Kapanen M et al. Diffusion-weighted magnetic resonance imaging for evaluation of salivary gland function in head and neck cancer patients treated with intensity-modulated radiotherapy. *Radiother Oncol* 2017; 122: 178–184.
96. Tenhunen M, Collan J, Kouri M et al. Scintigraphy in prediction of the salivary gland function after gland-sparing intensity modulated radiation therapy for head and neck cancer. *Radiother Oncol* 2008; 87: 260–267.